

1 Reinvestigating the fossil leaf *Welwitschiophyllum brasiliense* Dilcher et  
2 al., 2005, from the Lower Cretaceous Crato Formation of Brazil

3 Emily A. Roberts<sup>1, 2\*</sup>, Robert F. Loveridge<sup>1</sup>, Jörg Weiß<sup>3</sup> David M. Martill<sup>1</sup> and Leyla J. Seyfullah<sup>2</sup>

4 <sup>1</sup>School of the Environment, Geography and Earth Sciences, University of Portsmouth, Burnaby Road, Portsmouth,  
5 PO1 3QL, UK

6 <sup>2</sup>Department of Palaeontology, University of Vienna, Althanstraße 14, 1090 Vienna, Austria

7 <sup>3</sup> Mikroskopisches Kollegium Bonn, Helene-Lange-Strasse 25, 53757 Sankt Augustin, Germany

8 \*Corresponding author: Emily Roberts, [emily.roberts@port.ac.uk](mailto:emily.roberts@port.ac.uk)

9

10 **ABSTRACT**

11 The Lower Cretaceous Crato Formation of north-east Brazil yields a diverse plant assemblage. It has  
12 yielded many macrofossils thought to be related to the enigmatic gymnosperm group Gnetales,  
13 including the long leaf *Welwitschiophyllum brasiliense* Dilcher et al., 2005. This fossil plant is considered  
14 to be related to the extant gnetalean *Welwitschia mirabilis* Hooker, 1863, despite lacking many  
15 gnetalean characteristics. Presently, this macrophyte fossil is known only from detached leaves and  
16 much anatomical information is currently unavailable. The reproductive structures assigned to the  
17 family Welwitschiaceae in the Crato Formation, as well as several key morphological features of the  
18 leaves are currently thought to relate fossil *Welwitschiophyllum* to extant *Welwitschia*. These leaf  
19 characters include: isobilateral leaf form, triangular elongated leaf shape with a wide base, longitudinal  
20 splitting from a frayed leaf apex, numerous parallel veins and possible thickening of the epidermis.  
21 However, many of these leaf characteristics also occur in many other macrophytes, perhaps as a result  
22 of convergence. Anatomical and morphological data described here from fossil *Welwitschiophyllum*  
23 leaves is compared with extant *Welwitschia*. Our results show that *Welwitschiophyllum* can only be  
24 placed tentatively in Gnetales, as many of the features we report are not diagnostic, and may have  
25 resulted from convergent evolution (e.g., gum). Fossils with better anatomical preservation and the

26 reconstruction of the whole plant are really needed to better understand the affinities of  
27 *Welwitschiophyllum*.

28 Keywords: Crato Formation, Lower Cretaceous, Gnetales, *Welwitschia*, *Welwitschiophyllum*

29

### 30 **1. Introduction**

31 Early Cretaceous floras typically have a higher abundance of gymnosperms than seen in many  
32 floras today, where angiosperms (flowering plants) have become dominant following the Cretaceous  
33 Terrestrial Revolution (Lloyd et al., 2008). One gymnosperm group in particular that flourished during  
34 the Mesozoic was the Gnetales (Crane, 1996), today represented only by three genera that vary  
35 significantly in morphological appearance and habitat. *Ephedra* Linnaeus 1753 is a plant with reduced  
36 leaves, usually shrubby, although a few are small trees and climbers, and it has 50 species distributed in  
37 subtropical, arid and temperate environments (Kubitzki, 1990). *Gnetum* Linnaeus 1767 has 39 species,  
38 mostly lianas, but includes trees and shrubs, which are all broad leaved with pinnate-reticulate  
39 venation, and inhabiting sub-tropical to tropical environments (Ickert-Bond and Renner, 2016).  
40 *Welwitschia mirabilis* Hooker 1863 is a plant with only two elongated, strap-like leaves on the woody  
41 caudex and a large taproot, and is restricted to the Namib Desert with only one species. *W. mirabilis* is  
42 sometimes divided into subspecies *W. mirabilis* ssp. *mirabilis* and *W. mirabilis* ssp. *namibiana*  
43 (Leuenberger, 2001).

44 The Gnetales of the Mesozoic display a rich diversity not reflected in the extant genera (Rydin  
45 et al., 2006; Crane, 1996). This diversity is well documented in the Lower Cretaceous Crato Formation of  
46 north-east Brazil, where eight genera have been erected to date, and many more plants identified as  
47 gnetalean, are yet to be described (Rydin et al., 2003; Dilcher et al., 2005; Martill et al., 2007;  
48 Kunzmann et al., 2009; Kunzmann et al., 2011; Ricardi-Branco et al., 2013; Löwe et al., 2013). Four of  
49 these Crato Formation plant fossils are considered to be relatives of *Welwitschia*; the seedling *Cratonia*  
50 *cotyledon* Rydin et al., 2003, young paired cotyledon *Priscowelwitschia austroamericana* Dilcher et al.,  
51 2005, male reproductive strobili *Welwitschiostrobus murili* Dilcher et al., 2005, and the leaf taxon

52 *Welwitschiophyllum brasiliense* Dilcher et al., 2005. The diversity of these *Welwitschia* associated  
53 macro-remains are of interest, as its history is chiefly represented by pollen in the fossil record.

54 Other Lower Cretaceous macro-remains with possible Welwitschiaceae affinities are known  
55 from the United States, China, Mongolia, Russia, and Europe. These fossils include the reproductive  
56 structures *Gurvanella dictyoptera* Krassilov, 1982 (= *Chaoyangia liangii* Duan, 1998; Rydin et al., 2006),  
57 *Heerala antiqua* (Heer) Krassilov and Bugdaeva, 1988, *Angarolepis odorata* Krassilov and Bugdaeva,  
58 1988, *Eoantha zherikhinii* Krassilov, 1986, and the dispersed seeds, *Bicatia* Friis et al., 2014. *Drewria*  
59 *potomacensis* Crane and Upchurch, 1987 and *Conospermites hakeaefolius* Ettinghausen, 1867 are the  
60 only confirmed foliar remains of Welwitschiaceae found outside the Crato Formation.

61 *Welwitschiophyllum* is a rare occurrence of a non-cotyledonous foliar fossil assigned to  
62 Welwitschiaceae. They occur as distinctive detached leaves reaching up to ~850 mm in length. In order  
63 to better understand the relationship of this fossil taxon to *Welwitschia*, which previously was only  
64 based on morphological comparisons, we provide and review the *Welwitschiophyllum* anatomy based  
65 on thin sections and compare its histology to that of extant *Welwitschia*.

66

## 67 **2. Geological setting**

68 The Lower Cretaceous (~120 million years old) Crato Formation of north-east Brazil outcrops on  
69 the flanks of the Chapada do Araripe, in the Araripe Basin, mainly in the states of Ceará and  
70 Pernambuco (Batten, 2007; Martill, 2007) (Fig. 1). The best exposures are of anthropic origins (stone  
71 quarries) in the neighbourhood of Nova Olinda and Santana do Cariri in southern Ceará. All the fossils  
72 described here come from the quarries in this region. The formation comprises a heterolithic sequence  
73 of clays, silts and sands with conspicuous finely laminated limestones (Martill et al., 2007). The main  
74 fossil-bearing horizon, the Nova Olinda Member, is a composed of finely laminated limestone yielding a  
75 diverse and exceptionally preserved vertebrate, insect and plant assemblage (Martill et al., 2007).  
76 When found in the weathered limestone the plant fossils are preserved as orange-brown goethite  
77 compressions, but when found in the unweathered limestone they appear black; in both three-

78 dimensionality can be seen. The depositional environment is that of a saline lagoon with fresh water  
79 input with surrounding semi-arid to arid areas (Martill et al., 2007). Aridity is supported by the xeric  
80 adaptations of some of the flora (Mohr et al., 2006; Kunzmann et al., 2009; Mohr et al., 2015).

81

### 82 **3. Materials and methods**

83

84 *Fossil repositories:* The fossil material from the Crato Formation examined here comprises three  
85 isolated leaves of *W. brasiliense* Dilcher et al. 2005 (Specimens UERJ 13-P1, UERJ 14-P1, and UOP-PAL-  
86 MC0003). Specimens UERJ 13-P1, UERJ 14-P1 are accessioned at Rio Janeiro State University and UOP-  
87 PAL-MC0003 is accessioned at the University of Portsmouth.

88

89 *CITES Permit:* Analysis of extant *W. mirabilis* was performed on samples obtained on CITES permit No.  
90 152606.

91

92 *Petrographic thin sections:* To examine the fossil plant histology three petrographic thin sections from  
93 specimens UERJ 13-P1, UERJ 14-P1, and UOP-PAL-MC0003 were made. To avoid damage in the initial  
94 cutting and grinding stages the specimens were painted with thin layers of EpoThin II resin. The initial  
95 layer of resin was applied whilst the sample was heated on a hotplate to 80°C, it was then placed in  
96 a Struers Citovac vacuum chamber for 10 minutes and left overnight in a Heraeus Technomat pressure  
97 chamber to allow the resin to fully impregnate the material. Once the resin had cured the sample was  
98 cut using a Cutangrind saw made by Agate & General and a Buehler IsoMet Low Speed Precision Cutting  
99 Machine. Once cut, the surface was ground flat using 600 grade silicon carbide and water on a glass  
100 plate, and the sample was thoroughly dried then bonded with Epothin II to frosted glass using resin.  
101 Once the resin was cured, all excess material was cut away using a Buehler Petrothin machine leaving  
102 0.5 mm thick sample attached to the glass, which was then carefully ground down to 35-40 µm. The  
103 slide was then further ground down to the finished 30 µm (using 600 grade silicon carbide and water on

104 a glass plate) whilst the mineralogy was being periodically checked using a petrological microscope to  
105 ensure even thickness. These were examined using Leica DM750P and Zeiss Ax10 microscopes.

106

107 *Botanical thin sections:* Sections of *Welwitschia mirabilis* were fixed using AFE (Ethanol 70%,  
108 Formaldehyde 36% and acetic acid 99% - 90:5:5), 50 µm sections with Jung cylinder microtome, staining  
109 W3Asim II and examination with Leica DMLS microscope (Müller et al., 2011; Weiß, 2015).

110

111 *Paraffin sections:* Sections of *Welwitschia mirabilis* were fixed using ethanol (50%), formaldehyde (10%)  
112 glacial acetic acid (5%) and distilled water (35%) and then embedded in paraffin wax.

113

114 *Scanning electron microscopy:* SEM on fossil samples was undertaken on a Zeiss Evo Series NA10.  
115 Extant *Welwitschia mirabilis* samples were examined under variable pressure.

116

117 *Fossil gum extraction and Spectroscopic analysis :* The fossil amber-coloured material (from  
118 *Welwitschiophyllum* UERJ 13-P) was mechanically extracted from the matrix and the leaf fossil remains  
119 using sterile scalpel blades and dental picks from leaf ducts using a Leica EZ4W stereomicroscope. The  
120 extracted samples were washed in absolute alcohol to minimise contamination. The sample was then  
121 ground into a fine powder using a pre-autoclaved and pre-sterilised glass micro-mortar and pestle. The  
122 resulting powder was then further checked microscopically for any visible impurities, and none were  
123 seen. Analysis on the sample (UERJ 13-P1) was performed using FTIR spectroscopy on a *PerkinElmer*  
124 '*Spectrum 400*' spectrometer, fitted with an ATR sampling accessory (range 4000-550 cm<sup>-1</sup>, 32  
125 accumulations, 4 cm<sup>-1</sup> resolution). For ATR analyses a small amount of the sample was placed in 0.5 ml  
126 of water, which was heated to approximately 90°C for 10 minutes. A drop of the residual liquid was  
127 placed on the ATR crystal, and the water allowed to evaporate, leaving a film of the extracted material  
128 on the crystal surface. A spectrum was recorded (with 32 accumulations, to improve the quality of the  
129 data, due to the very small amount of material under analysis) and peaks were normalised. Care was

130 taken to thoroughly clean the ATR crystal between sample measurements using warm water and pure  
131 ethanol and allowed to dry. Test spectra were made to ensure no cross contamination was occurring  
132 between the measurement scans. A baseline correction for both analyses with reference points at 3715  
133 and 1800  $\text{cm}^{-1}$  was performed. The spectrograph was visualised using SpectraGryph 1.2.10 software.

134  
135 *Image processing:* Images were captured taken using Cannon EOS 80D and composed as combined  
136 figures using Inkscape. Fig. 1 was drawn in Inkscape. Fig. 2 is composed of single images taken and  
137 combined using Inkscape. Fig. 3A was stitched together to create an overview of the section, while Fig.  
138 3B-3E were processed in Inkscape. Fig. 4A, B were stitched together to create an overview of the section.  
139 Fig. 4C, D were processed in Inkscape. Fig. 5. was visualised in SpectraGryph 1.2.10 software. Fig. 6A was  
140 processed in Inkscape, Fig. 6B was stacked using Zerene Stacker from 30 single images taken with a  
141 Panasonic GX7, whilst Fig. 6C (three images) and 6D (five images) were stacked using Helicon Focus.

142

#### 143 **4. Results comparing *Welwitschiophyllum* and *Welwitschia***

144

##### 145 *4.1. Morphology and anatomy of fossil Welwitschiophyllum leaves*

146 *Welwitschiophyllum brasiliense* Dilcher et al., 2005 is a relatively common fossil leaf found in  
147 the Crato Formation. They are long (up to ~116 cm in length), lanceolate, detached leaves that taper to  
148 an acute apex and have a curved base (Fig. 2A). Where preserved, the leaves have a dense parallel  
149 venation (9-15 veins per cm). A single specimen comprising two apparently basally attached leaves that  
150 may be inferred as forming part of a rosette or other structure, was not available for study (Martill et  
151 al., 2007, pl. 27d). In some specimens the apex is frayed (Fig. 2B). *W. brasiliense* has also been recorded  
152 in association with the pterosaur *Ludodactylus*; it was first thought that the rigid and sharp leaf pierced  
153 the gular of the pterosaur leading to its eventual death (Frey et al., 2003; Martill et al., 2007, Fig. 17.4).  
154 An alternative theory is that this is in fact an abiotic association, due to the hyoid apparatus being  
155 preserved on top of the *Welwitschiophyllum* leaf, rather than wrapping around either side of the leaf

156 (Witton, 2017), which we deem less likely given the positioning of the leaf inside the mandibular  
157 apparatus.

158 Three specimens (Table 1, Fig. 2B–D) were available for detailed morphological and anatomical  
159 investigation for this study.

160

161 **Table 1. A summary of the three examined *Welwitschiophyllum* specimens.**

162	<b>Specimen</b>	<b>Length</b>	<b>Maximum</b>	<b>Apex</b>	<b>Preservation</b>
163			<b>width</b>		
164					
165	UERJ 13-P1	279 mm	44 mm at	Frayed	Leaf colour - black (from
166	(Fig. 2B)		its base		unweathered limestone).
167					
168	UERJ 14-P1	Leaf is incomplete (total length	52.5 mm	Missing	Leaf colour - black (from
169	(Fig. 2C)	unknown). Length of remaining	at its base		unweathered limestone). Leaf
170		portion is 482 mm.			partly covered by limestone
171					matrix.
172					
173	UOP-PAL-	Leaf is incomplete (total length	32.5 mm	Missing	Leaf colour - red-brown (from
174	MC0003	unknown). Length of remaining			weathered limestone). Leaf base
175	(Fig. 2D)	portion is 37 mm			is folded into the limestone.
176					
177					
178					

179 As the whole plant is unknown for *Welwitschiophyllum*, and considerable information on leaf  
180 morphology and anatomy is information unavailable (e.g., for the epidermis, stomata, internal leaf  
181 tissues and their arrangement), adaxial and abaxial surfaces are inferred from the curvature of the leaf  
182 base. The inferred adaxial surface here is defined as the surface on the incurved side of the leaf and the  
183 abaxial the opposite surface. *Welwitschiophyllum* sections display differences between the inferred  
184 adaxial and abaxial surfaces (Fig. 3A, B). The abaxial surface possesses flask shaped pits at regular  
185 intervals with spacing of 380  $\mu\text{m}$ , and depth of 125  $\mu\text{m}$ . In UOP-PAL-MC0003, these pits are infilled,  
186 with sediment (Fig. 3A, B). Although no stomata are seen, these regular pits are interpreted as possible  
187 stomatal crypts on the basis of their size and regular distribution throughout the abaxial leaf surface.  
188 Between the stomatal crypts raised sections of the leaf are highly fibrous (Fig. 3B), however, in all cases  
189 the cuticle and upper epidermis is not preserved.

190 The adaxial leaf surface lacks the stomatal crypts seen in the abaxial surface, and has thick  
191 fibres in bundles throughout the surface (Fig. 3A, B). These are interpreted as hypodermal fibres due to

192 their positioning and thick (20  $\mu\text{m}$ ), fibrous nature. No definite vascular tissue have been identified in  
193 any of the specimens, but 250  $\mu\text{m}$  wide voids (Fig. 3A, B) are here interpreted as the lacunae left by  
194 degraded vascular bundles. Neither accessory vascular bundles or lacunae of vascular bundles were  
195 identified.

196 Scanning electron microscopy (SEM) of the *Welwitschiophyllum* specimens revealed little detail  
197 as the leaf surfaces have been heavily mineralised and/or weathered away. However, one fossil leaf  
198 (UOP-PAL-MC0003) did retain some paradermal details (Fig. 3C, D). These include tube shaped  
199 structures that taper at the ends, connecting to each other (Fig. 3C, D) with holes perforating the  
200 structure (Fig. 3E). We interpret these structures as tracheids due to the tapering spindle shape of the  
201 connecting structures (Fig. 3C, D) and presence of pits present (Fig. 3E).

202 Transverse thin sections through the leaf show the variable amounts of anatomical details  
203 preserved in different leaves (Figs. 3A, 4A, 4B) and encroaching pyrite decay. Two thin sections of fossil  
204 *Welwitschiophyllum* leaves (UERJ 13-P1 and UERJ 14-P1) show adaxial amber-coloured ducts ranging in  
205 diameter from 75  $\mu\text{m}$  to 200  $\mu\text{m}$  wide (Fig. 4C, D). When analysed using FTIR and ATR they show a gum  
206 signal remarkably similar to that of extant *Welwitschia* gum (Fig. 5) (Roberts et al., 2020). In specimen  
207 UOP-PAL-MC0003 there are no remains of gum present, however, regular voids infilled with crystals  
208 towards the adaxial surface may represent ducts where the gum has been dissolved and infilled (Fig.  
209 3B). The arrangement of these regular ducts indicates that these were constituent within the leaf.

210

#### 211 4.2. Morphology and anatomy of leaves of extant *Welwitschia*

212 Despite *Welwitschia's* appearance of having many leaves it has only two perennial paired leaves  
213 (Fig. 6A) where the apices fray into 'thongs' (Hooker, 1863). The leaves are long, broad and coriaceous,  
214 and often split, giving the impression of separate leaves (Bornman et al., 1972). The parallel veined  
215 leaves can reach over 6 m in length (Hooker, 1863) and insert into a thick stem that has a robust  
216 corrugated periderm under the apex, which in mature specimens forms a distinctive 'terminal groove'  
217 (Hooker, 1863; Bornman et al., 1972). These two leaves are often strongly adaxially recurved. Below the



218 leaves the robust fibrous stem sits above the soil, and below it forms a massive root. *Welwitschia* is  
219 dioecious, where one plant bears either ovulate or staminate cones ~~or micro-strobili~~. Usually, although  
220 not always, these are adaxial to the leaves developing from the stem meristem (Bornman et al., 1972).

221 When thin sectioned notable features of *Welwitschia* (Fig. 6B) leaves are sunken stomata,  
222 hypodermal fibres and sclerenchymous fibres, all appearing both adaxially and abaxially. Thin sections  
223 of *Welwitschia* investigated here did not reveal evidence of gum ducts, but paraffin sections show an  
224 orange-brown coloured amorphous mass that lacks any cellular detail (Fig. 6C, D). The only instance of  
225 gum in the thin sections was found in a callus, again seemingly amorphous (Fig. 6E). We interpret these  
226 instances as traumatic gum production formed lysigenously.

227

## 228 5. Discussion

229 *Welwitschiophyllum* was originally placed in the Welwitschiaceae based on the isobilateral form  
230 of the leaves, possible thickening of the epidermis, triangular elongated leaf shape with a wide base,  
231 parallel equidistant first-order veins that are convergent near the apex, with some veins disappearing  
232 into the margin, plus longitudinal splitting from a frayed leaf apex, and somewhat thickened or creased  
233 mid-leaf area (Dilcher et al., 2005). We observed some of these features but not any possible thickening  
234 of the epidermis, as the preservation did not allow this. We also could not observe any thickened or  
235 creased mid-leaf area. The folded leaf specimen (UOP-PAL-MC0003) may have folded that way into the  
236 sediment due to a creased mid leaf area, but this is not evident in the thin sections.

237

### 238 5.1. Comparative anatomy of *Welwitschiophyllum* and *Welwitschia* leaves

239 The general morphology of *Welwitschiophyllum* leaves differ from those of the extant  
240 *Welwitschia* in a number of respects, including smaller fossil leaves, a lanceolate outline and a concave  
241 leaf base. *Welwitschiophyllum* is only found as detached leaves, and thus it is not possible to determine  
242 the leaf arrangement for the fossil taxon and compare it to the rather unique two-leaf arrangement of  
243 *Welwitschia* (Fig. 2 and Fig. 6). It is possible that the *Welwitschiophyllum* leaves were abscised or, as

244 suggested by Dilcher et al. (2005), that they were wrapped around a stem. *Welwitschiophyllum* leaves  
245 have distinct bases, whereas the very long, strap shaped, perennial leaves of *Welwitschia* originate  
246 inside the stem and are not abscised. Despite these clear differences in general morphology the plants  
247 do share some similarities in their long, thick leaves (growing to a considerable size) with first order  
248 parallel venation.

249 The parallel venation of *Welwitschiophyllum* is not, however, a convincing character to assign  
250 this fossil taxon leaf to Welwitschiaceae. Other fossil non-cotyledonous leaves (e.g. *Drewria* and  
251 *Conospermites*) assigned to Welwitschiaceae display two vein orders, first order parallel veins, plus a  
252 second order cross-venation with a chevron arrangement (Ettinghausen, 1867; Crane and Upchurch,  
253 1987). This more typical welwitschioid leaf venation is highly conspicuous in *Drewria* and *Conospermites*  
254 without the need for thin sectioning, unlike *Welwitschiophyllum* that clearly lacks accessory veins.

255 In the original description of *Welwitschiophyllum* the distinctive fraying of the leaf's apex was  
256 also considered to ally this fossil leaf to the extant *Welwitschia*: (Dilcher et al., 2005) (Fig. 2B). Fraying of  
257 the leaf in extant *Welwitschia* is often attributed to the wind (Bornman et al., 1972; Dilcher et al., 2005;  
258 Maneveldt and Seydlitz, 2007), but the phenomenon also occurs in glasshouse cultivated specimens  
259 where wind does not impact on the plant's development. Rather, it is thought that this fraying and  
260 damaged apices is a result of sun damage (Martens, 1971; Norbert Lehl, Vienna Palm House pers.  
261 comm., 2019, pers. Obs., EAR, LJS). As discussed by Dilcher et al. (2005) fraying seen in the fossil  
262 *Welwitschiophyllum* could have been a consequence of prolonged transport prior to deposition.  
263 Additionally, many extant leaves with a similar elongate-lanceolate morphology also display fraying at  
264 their apices e.g. *Yucca*, palms, *Cordyline* etc. Therefore, fraying of the leaf apex in *Welwitschiophyllum*  
265 cannot be considered a reliable characteristic allying it with *Welwitschia*.

266

## 267 5.2. Internal anatomy of *Welwitschiophyllum* and *Welwitschia* leaves

268 Unlike *Welwitschia*, thin sections of *Welwitschiophyllum* display significant differences in  
269 structure of the adaxial and abaxial surfaces, despite the limits of preservation shown in the prepared

270 materials presented here. *Welwitschia* has sunken stomata and bands of hypodermal fibres both  
271 adaxially and abaxially (Fig. 6B and Figures 1-2 of Rodin, 1958). *Welwitschiophyllum* has instead  
272 stomatal crypts abaxially, with gum ducts and bands of hypodermal fibres adaxially (Fig. 3B). These  
273 fibres have been interpreted as palisade cells by Biemann (2005). However, hypodermal fibres are more  
274 likely to be preserved than the palisade cells due to their dense fibrous nature that strengthens the leaf.  
275 The continuous fibres throughout the adaxial surface indicate that the leaf was quite rigid.

276 In Dilcher et al.'s (2005a) original discussion (but not their description) of *Welwitschiophyllum* it  
277 was suggested that the leaves may have had a thickened cuticle. No evidence for this is seen in our  
278 sections, but the epidermis and cuticle are not preserved in the specimens examined here.

279 In the sole transverse thin section illustrated by Biemann (2005, Figs. V.7, V.8, and V.12a), it is  
280 clear that the specimens studied have a similar level of preservation as our specimen UOP-PAL-  
281 MC0003, due to their similar weathered appearance and the reduced level of anatomical detail  
282 preserved. Biemann (2005) interprets what we believe to be stomatal crypts as stomatal cavities, then  
283 later (Fig. V.12) marks one cavity as a bundle of hypodermic fibres. Biemann (2005) also interprets the  
284 placement of vascular bundles, epidermis, and mesophyll, however, these structures are not obvious in  
285 the section illustrated, so we do not consider that the interpretation is completely supported by the  
286 images presented (see Biemann, 2005: Figs. V.7, V.8 and V.12a). Despite this, we do consider that the  
287 likely degraded remains of vascular bundles are in a similar position to the lacunae present in our in our  
288 sections, represented by what we interpret as degraded vascular bundles. Extant *Welwitschia* has  
289 numerous vascular bundles and accompanying accessory bundles inside the leaf tissue, (see here Fig.  
290 6B and Rodin, 1958), these accessory bundles are not present in our specimens, nor those described by  
291 Biemann (2005).

292 There are, however, some similarities in structure between *Welwitschiophyllum* and  
293 *Welwitschia* in thin sections, including the hypodermal fibres, tracheids and sunken stomata. The  
294 comparisons are limited because clear vascular tissue is not preserved in our specimens, nor in the  
295 section illustrated by Biemann (2005).

296 5.3. Gum inside *Welwitschiophyllum* and *Welwitschia* leaves

297 Recently the first example of gum found preserved in the fossil record was discovered in the  
298 leaves of *Welwitschiophyllum* (Roberts et al., 2020). FTIR analysis of this gum revealed it to be  
299 remarkably similar to that present in leaves of *Welwitschia* (Roberts et al., 2020). The spectra generated  
300 for the two gums are almost indistinguishable from each other and share key features in their spectra (a  
301 very large hydroxyl peak at  $\sim 3400\text{ cm}^{-1}$ , peak absence at  $1516\text{ cm}^{-1}$  and a very strong peak at  $1077\text{ cm}^{-1}$   
302 (Fig. 5, Roberts et al., 2020). Further characterization of the gum is planned. Elongate, thin gum ducts  
303 (lying parallel to the leaf axis) in *Welwitschiophyllum* are constituent within the leaf, i.e. they occur  
304 regularly, and even have a principle and a secondary duct arrangement (Fig. 4D and Roberts et al.,  
305 2020).

306 Gum, a water soluble polysaccharide, holds varying functional roles within plants, its  
307 constituent presence in *Welwitschiophyllum* could be food storage, structural support, wound sealing  
308 (to prevent water loss) or as a result of a pathology (e.g. fungal infection - gum ducts formed during  
309 injury followed immediately by fungal infection can form several tangential rows: Nair et al., 1980;  
310 Nussinovitch, 2010; BeMiller, 2014), although we regard the number of ducts more likely indicates a  
311 structural, storage or sealing role. In cases of traumatic gum formation, the gum appears unstructured  
312 and only very irregularly present (Fahn, 1988; Yamada, 2001). This is due to the different way the gum  
313 is initiated. In traumatic gum formation (gummosis) the cell wall (which forms the gum) breaks down  
314 and the subsequent amorphous gum appears at the point of the trauma. This is markedly different from  
315 constituent gum that is instead found organised into consistently placed ducts.

316 Different types of *Welwitschia* leaf sections allowed us to visualise both the anatomy and any  
317 potential gum. Our work shows that in all sections examined, regardless of sectioning/treatment  
318 method, gum ducts are absent. The only potential example of any kind of leaf gum we found is  
319 presented in Fig. 6C, which we have interpreted as a potential traumatic occurrence.

320 Historically, *Welwitschia* was thought to have constituent gum in both its leaves and stem  
321 (Sykes, 1911; Rodin, 1958). However, published accounts reveal conflicting reports of leaf gum in

322 *Welwitschia* (Table 2. Bertrand, 1874; Sykes, 1911). It is clear from careful analysis of the images and  
 323 text of the descriptions within these early studies that, in some cases, the likely erroneous  
 324 interpretation from Sykes (1911) and perhaps a misunderstanding of the description in Bertrand (1874)  
 325 was both accepted and propagated by subsequent authors (e.g. Takeda, 1913; Feustel, 1921; Rodin,  
 326 1958; Martens, 1971). Most illustrations and images of *Welwitschia* leaves lack gum ducts even when  
 327 they are mentioned within the text (Table 2, and see Feustel, 1921; Rodin, 1958; Martens, 1971). The  
 328 only two images detailing gum ducts are an incomplete drawing of a root with a ‘resinous gland’ half  
 329 drawn at the edge of the section by Bertrand (1874, plate 1, fig. 2) and another in a leaf section by  
 330 Sykes (1911, plate 17, fig. 1). We consider that the drawing by Sykes (1911, plate 17, fig. 1), is the  
 331 source of this confusion. Sykes’ illustration shows a cell-lined structure with the gum inside. However,  
 332 we cannot verify the presence, neither from our sections nor from the remaining literature, of a  
 333 secretory duct or blister in the leaves of *Welwitschia*. We believe that the interpretation of constituent  
 334 gum in *Welwitschia* by Sykes (1911) could instead be due to sectioning through a bleb of traumatically-  
 335 formed gum, and mistaking or assuming that the shape was contained within a cell-lined structure.

336

337 **Table 2. Citations and descriptions in the literature regarding *Welwitschia* gum.**

Literature	Terminology	Comments
Hooker (1863)	Gum	Lysigenous in the base (i.e. stem) and amorphous in the leaf. Gum not illustrated. See p. 12: ‘The gum which exudes from the trunk, peduncles, and various parts of the inflorescence, and which is also found abundantly in small cavities of the parenchyma of the leaf and trunk, is formed by the collenchymatous swelling and subsequent deliquescence of the cellular tissue, as is shown at Plate XII. figs. 14,15 [our note the illustration is of the stem tissue]. Occasionally the spicular cells are involved in the forming collenchyma, and, being similarly acted upon, their superficial coat of crystals becomes mixed up with the mass. The gum is dry, transparent, pale yellow-brown, inodorous, and insipid. See also p. 18–19: Towards the middle of the leaf is a thicker layer of ordinary parenchyma) having cell-walls without markings, and almost empty cavities, with a few spicula, and occasionally groups of cells transformed into amorphous gum (collenchyma)’ [our note: no gum illustrated].
Bertrand (1874)	Glandes résinifères	‘Resiniferous glands’ inside roots with illustration. See p. 7–8 and plate 1, fig. 2.

Literature	Terminology	Comments
De Bary (1884)	Mucilage sac	Doubts as to whether gum is constituent, but citing Hooker (1863). See fig. 187 [our note: an idealised <i>Welwitschia</i> section with possible sacs (labelled i, but not mentioned in caption)].
Sykes (1911)	Mucilage gland	Abaxial glands: see p. 181: a few mucilage glands occasionally appear on the lower side of the leaf. Only one illustration plate 17, fig. 1.
Takeda (1913)	Mucilage	Mentions mucilage canal presence. See p. 354–355: ‘The Mucilage Canal. In the adult leaf one often notices the presence of mucilage canals. These occur between bundles, and always on the phloem side. They are round in transverse section and comparatively short, varying from a few millimetres to as much as 1 cm or more, and they run parallel to the long axis of the leaf. They arise lysigenously owing to deliquescence of certain mesophyll cells. Similar mucilage canals occur in all parts of plants, except in a very young seedling’. [our note: no gum illustrated].
Feustel (1921)	Schleimkanäle	Translated from p. 239: ‘Mucous channels are often found in the adult leaf. Lies between bundles, always on the phloem [our note: abaxial] side. In cross section they show roundish diameter and are proportionate short, but varying from a few millimeters to 1 cm and more. They run parallel to the longitudinal axis of the leaf. Lysogenic origin’. [our note: no gum illustrated].
Rodin (1958)	Gum canals	Occasionally gum canals appear in the leaves mature plants. Also notes, gum canals always occur between vascular bundles on the lower side of the leaf adjacent to the phloem, as previously noted by Feustel (1921). Gum not illustrated.
Martens (1971)	Canaux lysigènes (gommes ou mucilages)	We translate p. 96: ‘Secretory tissues are the products of lysogenic canals with gum or mucilage occurring between bundles, and always on the phloem side (Sykes, 1911)’. No gum illustrated.

338

#### 339 5.4. Limits of preservation in *Welwitschiophyllum*

340           The preservation of *Welwitschiophyllum* impacts what can be observed. The best anatomical  
341 preservation comes counterintuitively from a weathered specimen UOP-PAL-MC0003, whereas the  
342 specimens (UERJ 13-P1 and UERJ 14- P1) that contain gum are found as unweathered specimens and  
343 appear to lack anatomical detail due to slight compaction and pyritisation. That gum is preserved in the  
344 unweathered material is more likely because it has undergone significantly less (or even none) meteoric  
345 weathering. Clearly, the unweathered specimens still had surrounding tissue intact protecting the  
346 highly water soluble gum. However, we cannot yet satisfactorily explain why the apparent better  
347 anatomical preservation occurs in weathered material, although we have been only permitted to  
348 section a few leaves.

349 The lack of vascular tissue present in the thin sections could be due to the high water content  
350 of the vessels, which are easily pyritised and thus the definition of the vascular tissue was lost due to  
351 mineral overgrowth. Conversely, hypodermal fibres are more likely to be preserved due to their dense  
352 fibrous nature. Despite the absence of xylem elements in thin sections under SEM, tracheids with pits  
353 can be seen (Fig. 3C, D and E). This preservation could be due to tracheids having a heavily lignified,  
354 three-layered secondary cell wall that is resistant to degradation, allowing their survival even though  
355 they are water conducting (Friedman and Cook, 2000).

356

#### 357 5.5. Possible convergent features of *Welwitschiophyllum* and *Welwitschia* leaves

358 While *Welwitschiophyllum* shares some morphological and anatomical characteristics with  
359 *Welwitschia* leaves, these also occur in many other arid-adapted plants. In particular, stomatal crypts  
360 are often found in arid-adapted plants, where it is thought they facilitate diffusion of CO<sub>2</sub> from the  
361 abaxial surface to the adaxial surface in thicker leaves, and lessen the exposure of the stomata to  
362 environmental conditions (Hassiotou et al., 2009). *Welwitschiophyllum* was a coriaceous leaf and  
363 thought to have lived in an arid habitat, where stomatal crypts would be beneficial by reducing the  
364 distance of CO<sub>2</sub> diffusion to the adaxial surface of the leaf. Many plants with stomatal crypts carry them  
365 on the abaxial surface of the leaf (Hassiotou et al., 2009; Roth-Nebelsick et al., 2009; Goldenberg et al.,  
366 2013), thus supporting our identification of abaxial and adaxial surfaces in *Welwitschiophyllum*.

367 Other features of *Welwitschiophyllum* that could be considered convergent include: coriaceous  
368 leaves, parallel venation, and a curved base. These can be seen in various fossil leaves: *Dracaena*  
369 *tayfunii* Denk et al., 2014, *Desmiophyllum gothanii* Florin, 1936, *Protoyucca shadishii* Tidwell and  
370 Parker, 1990, *Paracordyline* Conran and Christophel, 1998, *Pandanites* Tuzson, 1913, *Doryanthites*  
371 Berry, 1914, as well as numerous extant flora. The morphological similarity of *Welwitschiophyllum* to  
372 many other fossil leaves requires further investigation to determine botanical affinity.

373 Parallel leaf venation (without a midrib) as seen in *Welwitschiophyllum* is relatively common  
374 today in some monocots such as the Agavoidieae (e.g., *Agave*, *Yucca*) and across some Poales (which

375 includes the Bromeliaceae and Poaceae). Monocots are reported from the Crato Formation, but are  
376 quite distinct in their leaf shape and venation: *Spixiarum* Coiffard et al., 2013, *Cratolirion bognerianum*  
377 Coiffard et al., 2019, both having two vein orders.

378         Based on our new data we suggest that the affinity of the plant to which *Welwitschiophyllum*  
379 leaves belong is still unclear, since morphologically and anatomically many features observed could  
380 have resulted from convergence. There are some key differences including likely abscised, smaller fossil  
381 leaves, compared to perennial and ever-growing *Welwitschia* leaves and the differentiation between  
382 the abaxial and adaxial sides of the fossil leaf, but not in *Welwitschia* leaves. What is striking, however,  
383 is the presence of gum in both plants. However, even here there are clear differences. There are the  
384 regularly occurring gum ducts in *Welwitschiophyllum*, but possibly only traumatic gum blebs found in  
385 *Welwitschia* leaves. Based on the balance of the evidence so far, and until a whole plant can be fully  
386 reconstructed, we are still tentative with the definitive placement of *Welwitschiophyllum* in the  
387 Gnetales.

388

## 389 **6. Conclusion**

390         The original description (Dilcher et al., 2005) of *Welwitschiophyllum* related it to *Welwitschia*  
391 using the following characteristics: the isobilateral form of the leaves, possible thickening of the  
392 epidermis, triangular elongated leaf shape with a wide base, longitudinal splitting from a frayed leaf  
393 apex and numerous parallel veins. This study has shown that *Welwitschiophyllum* shares some key  
394 features with extant *Welwitschia*, i.e., having long, coriaceous, parallel veined leaves that produce gum  
395 and the presence of hypodermal fibres. However, there are some notable differences such as in the  
396 abaxial placement of stomatal crypts and solely adaxial hypodermal fibres seen in the fossil, whereas  
397 the extant plant has these on both sides of the leaf. There is no preserved evidence of epidermal  
398 thickening in the fossil leaves examined here, unlike that in *Welwitschia*. The method of gum  
399 production also differs between the two taxa, with *Welwitschiophyllum* having constituent gum ducts  
400 and *Welwitschia* amorphous traumatic gum formation. The frayed apex, present in many leaf species, is



401 not considered a dependable character. These characteristics used to define the botanical affinity of  
402 *Welwitschiophyllum* to *Welwitschia* must be used with caution, as they could be the result of  
403 convergence. Whilst the new anatomical data of *Welwitschiophyllum* revealed more detail than  
404 previously known and strengthening the likelihood of this plant belonging to an arid environment, it  
405 cannot yet definitively determine the relationship of *Welwitschiophyllum* to *Welwitschia*.

406

#### 407 **Acknowledgements**

408 We warmly thank the two anonymous reviewers whose constructive comments strengthened the  
409 paper and the support from our editor Dr Koutsoukos. We would like to thank Dr Anthony Hitchcock,  
410 Karin Behr and Benjamin Festus (SANBI, Pretoria, SA) and Michael Plewka (Gevelsberg) for assistance  
411 obtaining CITES permits and supplying *Welwitschia* samples. Norbert Lehl (Vienna Palm House) is  
412 thanked for his expertise on *Welwitschia*. Geoff Long (University of Portsmouth) kindly produced thin  
413 sections, while at the University of Portsmouth Elaine Dyer and Joe Dunlop assisted with scanning  
414 electron microscopy and Richard Hing helped with photography. Professor Christa Hofmann and Dr  
415 Hugh Rice are thanked for the *Welwitschia* image (University of Vienna. Support for LJS provided by the  
416 German Research Foundation (DFG), project number SE2335/3-1.

417

418 **Author contributions:** DMM, LJS and RFL devised the project, DMM and RFL undertook the fieldwork in  
419 Brazil. EAR, JW, RFL and LJS prepared the material. Interpretation was by EAR, and LJS. The paper was  
420 written by EAR, LJS, RFL, DMM, and JW.

421

422 **Competing interests:** No competing interests.

423

424 **Declaration of interest:** None.

425

426

427 **References**

- 428 Batten, D.J., 2007. Spores and pollen from the Crato Formation: biostratigraphic and palaeoenvironmental  
429 implications. In: Martill, D.M., Bechly, G., Loveridge, R.F. (Eds.), *The Crato Fossil Beds of Brazil—Window*  
430 *into an Ancient World*. Cambridge University Press, Cambridge, 566–573.
- 431 BeMiller, J.N., 2014. Plant gums. *Essential for Life Science* John Wiley and Sons Ltd, Chichester, pp. 661.
- 432 Berry, E.W., 1914. The Upper Cretaceous and Eocene floras of South Carolina and Georgia. U.S. Geological  
433 Survey Professional Paper, 84:1–200.
- 434 Bertrand, C.E. 1874. Anatomie des gnetacees et des coniferes. *Annales des sciences naturelles Botanique*  
435 20, 5–153.
- 436 Biemann, E.P.G.E., 2005. Angiospermas eocretáceas do Membro Crato (Formação Santana, Bacia do  
437 Araripe, NE do Brasil): Revisão taxonômica de *Welwitschiophyllum brasiliense* Dilcher, Bernardes-de-  
438 Oliveira, Pons et Lott, 2005. Programa de Pós-Graduação em Análise Geoambiental, Universidade  
439 Guarulhos, Dissertação de Mestrado, pp. 81. (Masters Dissertation, in Portuguese).
- 440 Bornman, C.H., Elsworthy, J.A., Butler, V., Botha, C.E.J., 1972. *Welwitschia mirabilis*: observations on  
441 general habit, seed, seedlings, and leaf characteristics. *Madoqua* II 1, 53–66.
- 442 Buehler. 2015. Preparation of petrographic thin sections. Buehler, Illinois Tool Works Inc. 1(3): 1–2.
- 443 Coiffard, C., Mohr, B.A.R., Bernardes-de-Oliveira, M.E.C., 2013. The Early Cretaceous Aroid, *Spixiarum kipea*  
444 gen. et sp. nov., and implications on early dispersal and ecology of basal monocots. *Taxon* 62, 997–  
445 1008.
- 446 Coiffard, C., Kardjilov, N., Manke, I., Bernardes-de-Oliveira, M.E.C., 2019. Fossil evidence of core monocots  
447 in the Early Cretaceous. *Nature Plants* 5, 691–696.
- 448 Conran, J.G., Christophel, D.C., 1998. *Paracordyline aureonemoralis* (Lomandraceae): an Eocene  
449 monocotyledon from Adelaide, South Australia. *Alcheringa* 22, 351–359.
- 450 Crane, P.R., Upchurch, G.R., 1987. *Drewria potomacensis* gen. et sp. nov., an Early Cretaceous member of  
451 Gnetales from the Potomac Group of Virginia. *American Journal of Botany* 74, 1722–1736.
- 452 Crane, P.R., 1996. The fossil history of the Gnetales. *International Journal of Plant Sciences* 157, 50–57.

453 De-Bary, A., 1884. Comparative anatomy of the vegetative organs of the phanerogams and  
454 ferns. (English translation by F. O. Bower and D. H. Scott.) Oxford.

455 Denk, T., Güner, H.T., Grimm, G.W., 2014. From mesic to arid: leaf epidermal features suggest  
456 preadaptation in Miocene dragon trees (*Dracaena*). *Review of Palaeobotany and Palynology* 200, 211–  
457 228.

458 Dilcher, D.L., Bernardes de Oliveira, M.E.C., Pons, D., and D, Lott, T.A., 2005. Welwitschiaceae from the  
459 Lower Cretaceous of Northeastern Brazil. *American Journal of Botany* 92, 1294–1310.

460 Duan, S.Y., 1998. The oldest angiosperm—a tricarpaceous female reproductive fossil from Western Liaoning  
461 Province, NE China. *Science in China (Series D)* 41, 14–20.

462 Ettingshausen, V., 1867. Die Kreideflora von Niederschona. *Sitzungsberichte der Kaiserlichen Akademie der*  
463 *Wissenschaften in Wien, Math C1.* 55, 235–264.

464 Fahn, A., 1988. Secretory tissues in vascular plants. *New Phytologist* 108, 229–257.

465 Feustel, H., 1921. Anatomie und Biologie der Gymnospermen Blätter. Beihefte zum botanischen  
466 *Centralblatt* 38, 235–244.

467 Florin, R., 1936. Die fossil en Ginkgophyten von Franz-Joseph Land nebst Erörterungen tiber vermeintliche  
468 *Cordaitales* mesozoischen Alters.I. Spezieller Teil. *Palaeontographica* 81, 1–173.

469 Frey, E., Martill, D.M., Buchy, M., 2003. A new crested ornithocheirid from the Lower Cretaceous of  
470 northeastern Brazil and the unusual death of an unusual pterosaur. In: Buffetaut. E., Mazin, J.M. (Eds.)  
471 *Evolution and Palaeobiology of Pterosaurs.* Geological Society, London, Special Publications 217, 55–63.

472 Friedman, W.E., Cook, M.E., 2000. The origin and early evolution of tracheid in vascular plants: integration  
473 of palaeobotanical and neobotanical data. *Philosophical Transactions of the Royal Society of London B*  
474 355, 857–868.

475 Friis, E.M., Pedersen, K.R., Crane, P.R., 2014. Welwitschioid diversity in the Early Cretaceous: evidence  
476 from fossil seeds with pollen from Portugal and eastern North America. *Grana* 53, 175-196.

477 Goldenberg, R., Meirelles, J., Amano, E., 2013. *Mouriri morleyii* sp. nov. (Melastomataceae) from Brazil,  
478 with notes on its foliar stomatal crypts. *Nordic Journal of Botany* 31, 321–325.

479 Hassiotou, F., Evans, J.R., Ludwig, M., Veneklaas, E.J., 2009. Stomatal crypts may facilitate diffusion of CO<sub>2</sub>  
480 to adaxial mesophyll cells in thick sclerophylls. *Plant, Cell and Environment* 32, 1596–1611.

481 Hooker, J.D., 1863. On *Welwitschia*, a new genus of Gnetaceae. *Transactions of the Linnean Society of*  
482 *London* 24, 1–48.

483 Ickert-Bond, S.M., Renner, S.S., 2016. The Gnetales: recent insights on their morphology, reproductive  
484 biology, chromosome numbers, biogeography, and divergence times. *Journal of Systematics and*  
485 *Evolution* 54, 1–16.

486 Krassilov, V.A., 1982. Early Cretaceous flora of Mongolia. *Palaeontographica B* 181, 1–43.

487 Krassilov, V.A., 1986. New floral structure from the Lower Cretaceous of Lake Baikal area. *Review of*  
488 *Palaeobotany and Palynology* 47, 9–16.

489 Krassilov, V.A., Bugdaeva, E.V., 1988. Gnetalean plants from the Jurassic of Ust-Balej, East Siberia. *Review*  
490 *of Palaeobotany and Palynology* 53, 359–374.

491 Kubitzki, K., 1990. Welwitschiaceae. In: Kramer, K.U., Green, P.S. (Eds.), *The families and genera of vascular*  
492 *plants, Volume 1, Pteridophytes and Gymnosperms*, Springer-Verlag, Berlin, Germany, pp. 387–391.

493 Kunzmann, L., Mohr, B.A.R., Bernardes-de-Oliveira, M.E.C., 2009. *Cearania heterophylla* gen. nov. et sp.  
494 nov., a fossil gymnosperm with affinities to the Gnetales from the Early Cretaceous of northern  
495 Gondwana. *Review of Palaeobotany and Palynology* 158, 193–212.

496 Kunzmann, L., Mohr, B.A.R., Wilde, V., Bernardes-de-Oliveira, M.E.C., 2011. A putative gnetalean  
497 gymnosperm *Cariria orbiculiconiformis* gen. nov. et spec. nov. from the Early Cretaceous of northern  
498 Gondwana. *Review of Palaeobotany and Palynology* 165, 75–95.

499 Leuenberger, B.E., 2001. *Welwitschia mirabilis* (Welwitschiaceae), male cone characters and a new  
500 subspecies. *Willdenowia* 31, 357–381.

501 Linnaeus, C., 1753. *Species plantarum* vol. 2. *Impensis Laurentii Salvii, Holmiae*, pp. 640.

502 Linnaeus, C., 1767. *Mantissa plantarum*. *Impensis Laurentii Salvii, Stockholm*.

503 <http://dx.doi.org/10.5962/bhl.title.69083>.

504 Lloyd, G.T., Davis, K.E., Pisani, D., Tarver, J.E., Ruta, M., Sakamoto, M., Hone, D.W., Jennings, R., Benton, M.  
505 J., 2008. Dinosaurs and the Cretaceous Terrestrial Revolution. *Proceedings of the Royal Society, B*.  
506 275(1650), 2483–2490. doi: 10.1098/rspb.2008.0715.

507 Löwe, S.A., Mohr, B.A.R., Coiffard, C, Bernardes de Oliveira, M.E.C., 2013. *Friedsellowia gracilifolia* gen.  
508 nov. et sp. nov. a new gnetophyte from the Lower Cretaceous Crato Formation (Brazil).  
509 *Palaeontographica Abteilung B, Palaeophytologie Palaeobotany-Palaeophytology* 289, 139–177.

510 Maneveldt, G.W., Von Seydlitz, A., 2007. Encounters in the Namib Desert. *Veld and Flora* 93, 36–41.

511 Martens, P., 1971. Les gnetophytes. *Handbuch der Pflanzenanatomie*. Vol 12, pt 2. Gebruider Borntraeger,  
512 Berlin, Germany pp. 295.

513 Martill, D.M., 2007. The geology of the Crato Formation. In: Martill, D.M., Bechly, G., Loveridge, R.F. (Eds.),  
514 *The Crato Fossil Beds of Brazil—Window into an Ancient World*. Cambridge University Press, Cambridge,  
515 8–24.

516 Martill, D.M., Bechly, G., Loveridge, R., 2007. *The Crato Fossil Beds of Brazil. Window into an Ancient*  
517 *World*. Cambridge University Press, Cambridge, pp. 625.

518 Mohr, B.A.R., Bernardes de Oliveira, M.E.C., Barale, G., Ouaja, M., 2006. Palaeogeographic distribution and  
519 ecology of *Klitzschophyllites*, an early Cretaceous angiosperm in southern Laurasia and northern  
520 Gondwana. *Cretaceous Research* 27, 464–472.

521 Mohr, B.A.R., Bernardes-de-Oliveira, M.E.C., Loveridge, R.F., Pons, D., Sucerquia, P.A., Castro-Fernandes,  
522 M.C., 2015. *Ruffordia goeppertii* (Schizaeales, Anemiaceae)- A common fern from the Lower Cretaceous  
523 Crato Formation of northeast Brazil. *Cretaceous Research* 54, 17–26.

524 Müller, R-D, Weiß, J., 2011, Wacker für alle - neue Simultanfärbungen auf Basis der W3A Färbung von  
525 Robin Wacker. [www.mikroskopie-bonn.de](http://www.mikroskopie-bonn.de); [http://mikroskopie-](http://mikroskopie-bonn.de/bibliothek/botanische_mikrotechnik/162.htm)  
526 [bonn.de/bibliothek/botanische\\_mikrotechnik/162.htm](http://mikroskopie-bonn.de/bibliothek/botanische_mikrotechnik/162.htm)

527 Nair, G.M., Patel, K.R., Shah, J.J., Pandalai, R.C., 1980. Effect of ethephone (2-chloroethyl phosphonic acid)  
528 on gummosis in the bark of *Azadirachta indica* A. Juss. *Indian Journal of Experimental Biology* 18, 500–  
529 503.

530 Nussinovitch, A., 2010. Plant gum exudates of the World: source, distribution, properties and applications.  
531 CRC Press, Taylor and Francis Group, United States of America, pp. 401.

532 Ricardi-Branco F., Torres M., Tavares S.S., De Souza Carvalho I., Tavares P.G.E., Campos A.C.A., 2013.  
533 *Itajuba yansanae* gen. and sp. nov. of Gnetales, Araripe Basin (Albian–Aptian) in Northeast Brazil. In:  
534 Zhang Y., Ray P., (Eds.) Climate change and regional/local responses. Rijeka: InTech, 187–205.

535 Rodin, R.J., 1958. Leaf Anatomy of *Welwitschia*. II. A Study of mature Leaves. American Journal of Botany  
536 45, 96–103.

537 Roberts, E.A., Seyfullah, L.J., Loveridge, R.F., Garside, P., Martill, D.M., 2020. Cretaceous gnetalean yields  
538 first preserved plant gum. Scientific Reports 10, 3401.

539 Roth-Nebelsick, A., Hassiotou, F., Veneklaas, E.J., 2009. Stomatal crypts have small effects on transpiration:  
540 a numerical model analysis. Plant Physiology 151, 2019–2027.

541 Rydin, C., Mohr, B.A.R., Friis, E.M., 2003. *Cratonia cotyledon* gen. et sp. nov.: a unique Cretaceous seedling  
542 related to *Welwitschia*. Proceedings of the Royal Society London Series B Biological Letter 270, 29–32.

543 Rydin, C., Wu, S.Q., Friis, E.M., 2006. *Liaoxia* Cao et S.Q. Wu (Gnetales): ephedroids from the Early  
544 Cretaceous Yixian Formation in Liaoning, northeastern China. Plant Systematics and Evolution 262, 239–  
545 265.

546 Sykes, M.G., 1911. The anatomy and morphology of the leaves and inflorescences of *Welwitschia mirabilis*.  
547 Philosophical Transactions of the Royal Society of London, series B 201, 179–226.

548 Takeda, H., 1913. Some points in the anatomy of the leaf of *Welwitschia*. Annals of Botany 27, 347–357.

549 Tidwell, W.D., Parker, L.R., 1990. *Protoyucca shadishii* gen. et sp. nov., An arborescent monocotyledon  
550 with secondary growth from the Middle Miocene of Northwestern Nevada, U.S.A. Review of  
551 Palaeobotany and Palynology 62, 79–95.

552 Tuzson, J., 1913. Adatok Magyarország fosszilis flórájához Magyarország fosszilis flórájához (Additamenta  
553 ad floram fossilem Hungariae III). A magyar királyi földtani intézet évkönyve 21, 209–233.

554 Weiß, J., 2015. Die Welwitschie (*Welwitschia mirabilis*), Mikroskopisches Kollegium Bonn,  
555 <http://mikroskopie-bonn.de/bibliothek/botanik/137.html>.

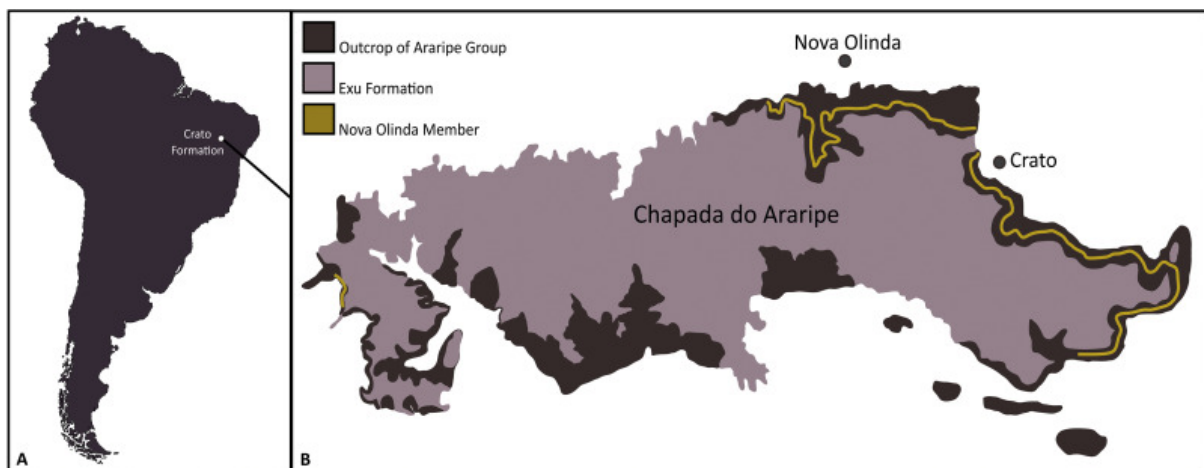
556 Witton, M.P., 2017. Pterosaurs in Mesozoic food webs: a review of fossil evidence. In: Hone, D.W.E.,  
557 Witton, M.P., Martill, D.M. (Eds.) *New Perspectives on Pterosaur Palaeobiology*. Geological Society,  
558 London, Special Publications 455, 7–23.

559 Yamada, T., 2001. Defense mechanisms in the sapwood of living trees against microbial infection. *Journal*  
560 *of Forest Research* 6, 127–137.

561

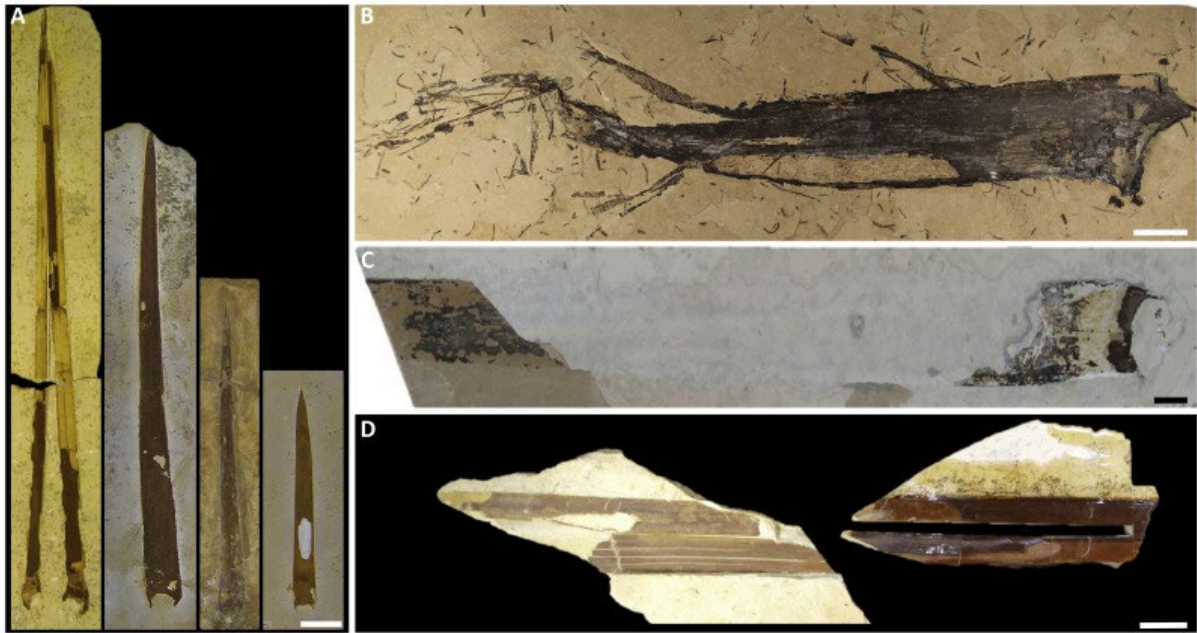
562

563 **Figures**



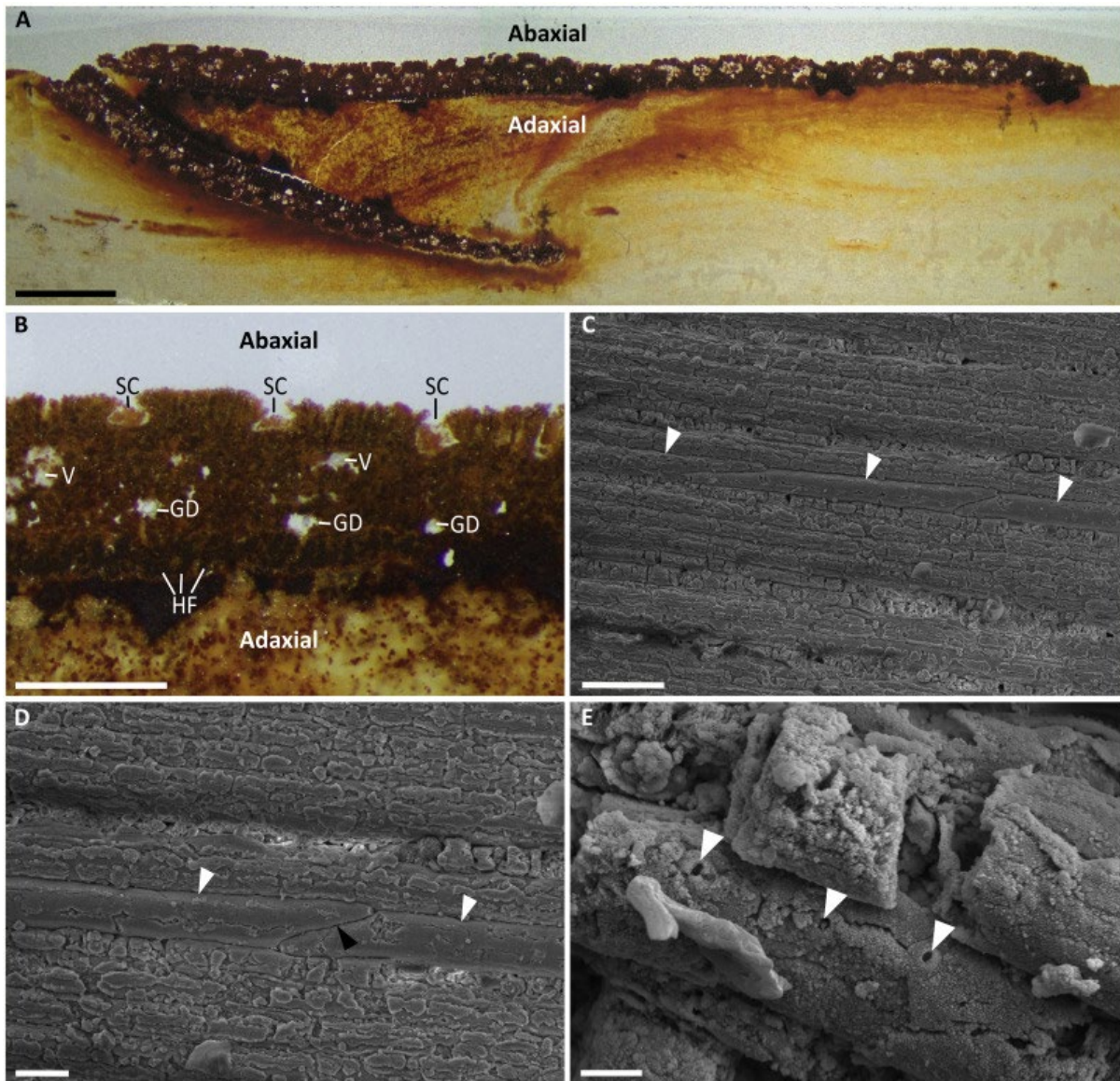
564

565 **Fig. 1.** Fig. 1. Locality map. (A) Map of South America with the location of the Crato Formation (north-east  
566 Brazil) marked. (B) A detailed outline of the Chapada do Araripe, and the outcrop of the Araripe Group  
567 (comprising of Ipubi, Crato and Rio da Batateiras formations), the Exu Formation and the Nova Olinda  
568 Member (the fossil-bearing horizon of the Crato Formation). Labelled spots indicate towns.

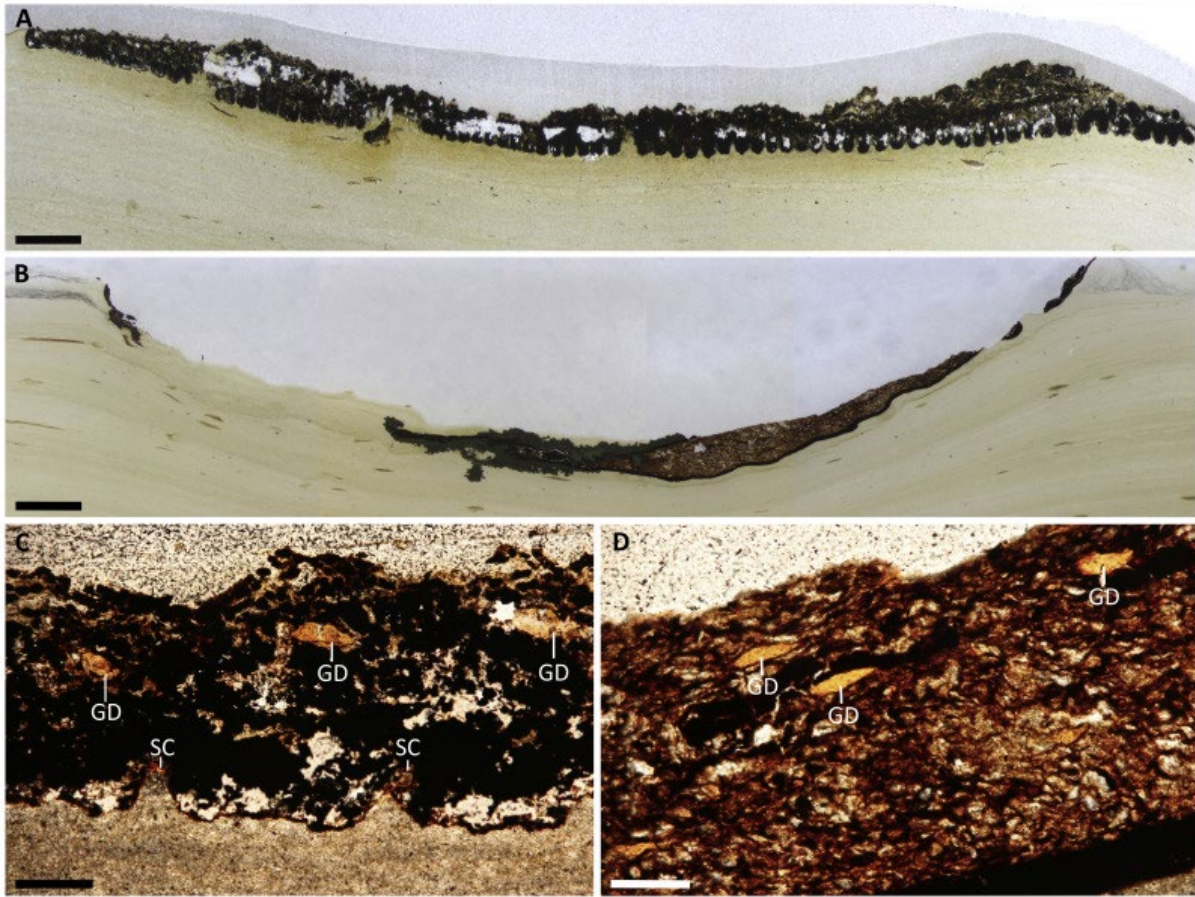


569  
570 **Fig. 2.** The fossil leaf taxon *Welwitschiophyllum brasiliense*. (A) Specimens of *Welwitschiophyllum* leaves  
571 displaying a range of sizes. (B) Unweathered specimen with frayed apex (UERJ 13-P1). (C) An  
572 incomplete, unweathered specimen that has been partially covered in sediment (UERJ 14-P1). (D)  
573 Incomplete weathered specimen that has folded over in the sediment (UOP-PAL-MC0003). Scale bar  
574 represents 80 mm (A) and 20 mm (B, C, D).





575  
 576 **Fig. 3.** Thin section and SEM images from a folded *Welwitschiophyllum brasiliense* specimen (UOP-PAL-  
 577 MC0003). This specimen is orientated with the abaxial leaf surface uppermost. (A) Thin section  
 578 overview with abaxial and adaxial surfaces labelled (B) Thin section showing the anatomy preserved:  
 579 SC, stomatal crypts; V, degraded vascular tissue; GD, weathered out gum duct; HF, hypodermal fibres,  
 580 abaxial and adaxial surfaces labelled. (C) SEM image of connecting tracheids (tracheids indicated using  
 581 white arrow heads). (D) SEM image showing the typical way in which tracheids connect (tracheids  
 582 indicated using white arrow heads and the connection indicated using black arrow heads). (E) SEM of  
 583 the pits on a tracheid indicated using white arrow heads. Scale bars represent 2 mm (A), 500  $\mu$ m (B),  
 584 100  $\mu$ m (C), 30  $\mu$ m (D), and 10  $\mu$ m (E).



585

586 **Fig. 4.** Thin sections from two specimens of *Welwitschiophyllum* (UERJ 13-P1 and UERJ 14-P1). (A)

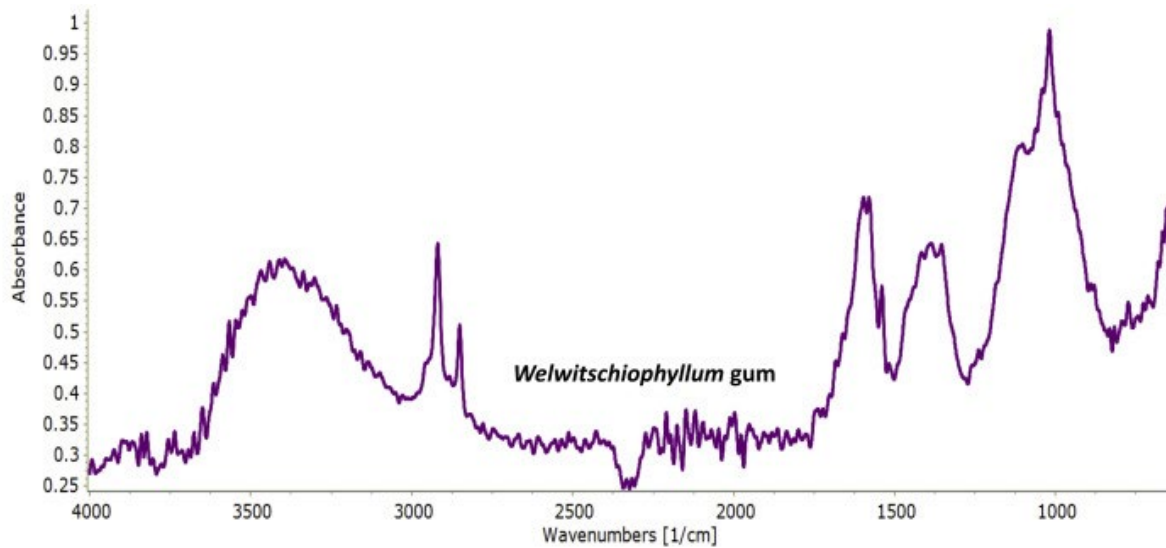
587 Overview thin section of UERJ 13-P1. (B) Overview thin section of UERJ 14-P1. (C) Detailed view of UERJ

588 13-P1 showing stomatal crypts (SC) and gum ducts with gum present inside (GD). (D) Detailed view of

589 UERJ 14-P1 gum ducts with gum still present inside. Scale bars represent 2 mm (A, B) and 200  $\mu$ m (C, D).

590

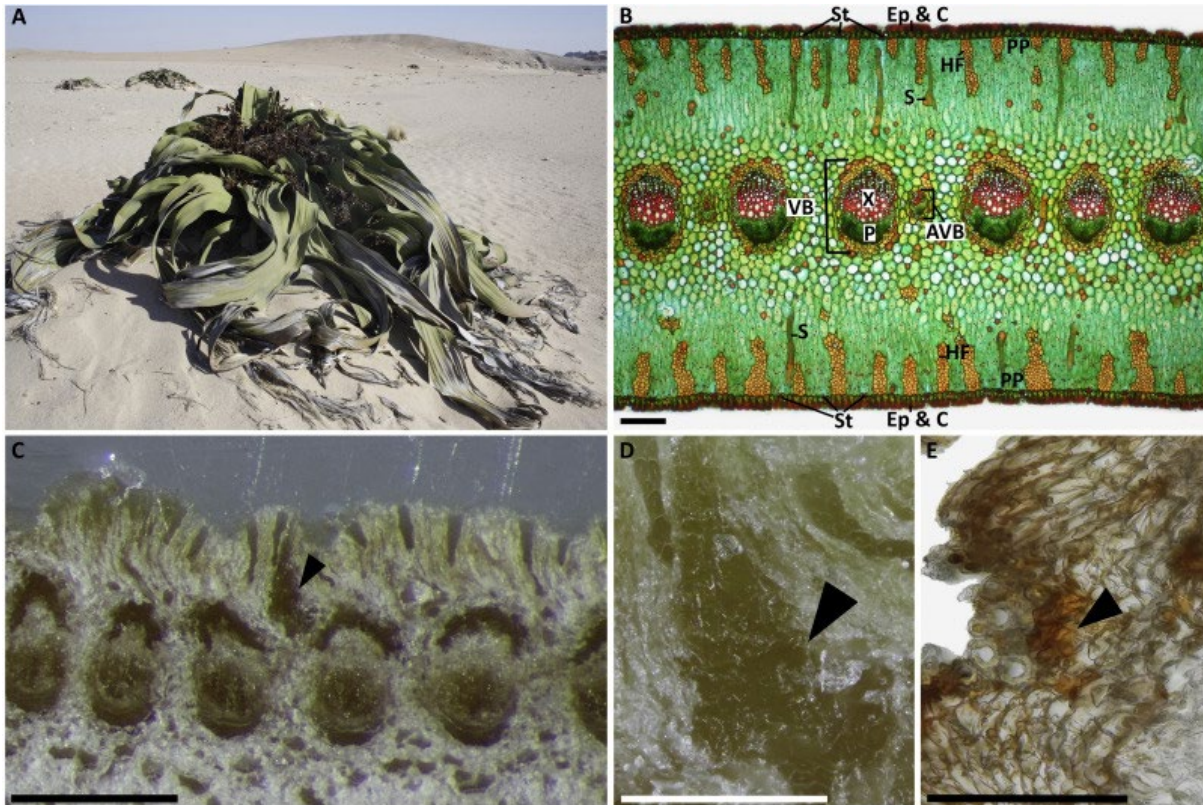
591



592  
593 **Fig. 5.** ATR spectrum of gum recovered from fossil *Welwitschiophyllum* leaves (Specimen UERJ P1-13),  
594 see Roberts et al., 2020.

595  
596  
597  
598  
599





600

601 **Fig. 6.** *Welwitschia mirabilis* overview, thin sections and paraffin sections. (A) Plant in the Namib Desert

602 (B) Stained thin section of a mature leaf showing anatomy: Ep & C, epidermis and cuticle; St, stomata;

603 PP, palisade parenchyma; HF, hypodermal fibres; S, sclerids; VB, vascular bundle; AVB, accessory

604 vascular bundle; X, xylem; P, phloem. (C) Paraffin section of mature leaf with black arrow indicating

605 traumatic formation of gum. (D) Detailed view of (C) with black arrow head indicating of the traumatic

606 gum showing its amorphous nature. (E) Traumatic gum formation indicated by a black arrow of a callus.

607 Scale bars represent 200  $\mu\text{m}$  (B), 500  $\mu\text{m}$  (C) 100  $\mu\text{m}$  (D) and 200  $\mu\text{m}$  (E). Photo credit for 5A to Drs

608 Christa Hofmann and Hugh Rice.

609